Evaluating uncertainties in regional climate simulations over South America at the seasonal scale

Silvina A. Solman & Natalia L. Pessacg

Climate Dynamics
Observational, Theoretical and Computational Research on the Climate System

ISSN 0930-7575
Volume 39
Combined 1-2

Clim Dyn (2012) 39:59-76
DOI 10.1007/s00382-011-1219-6

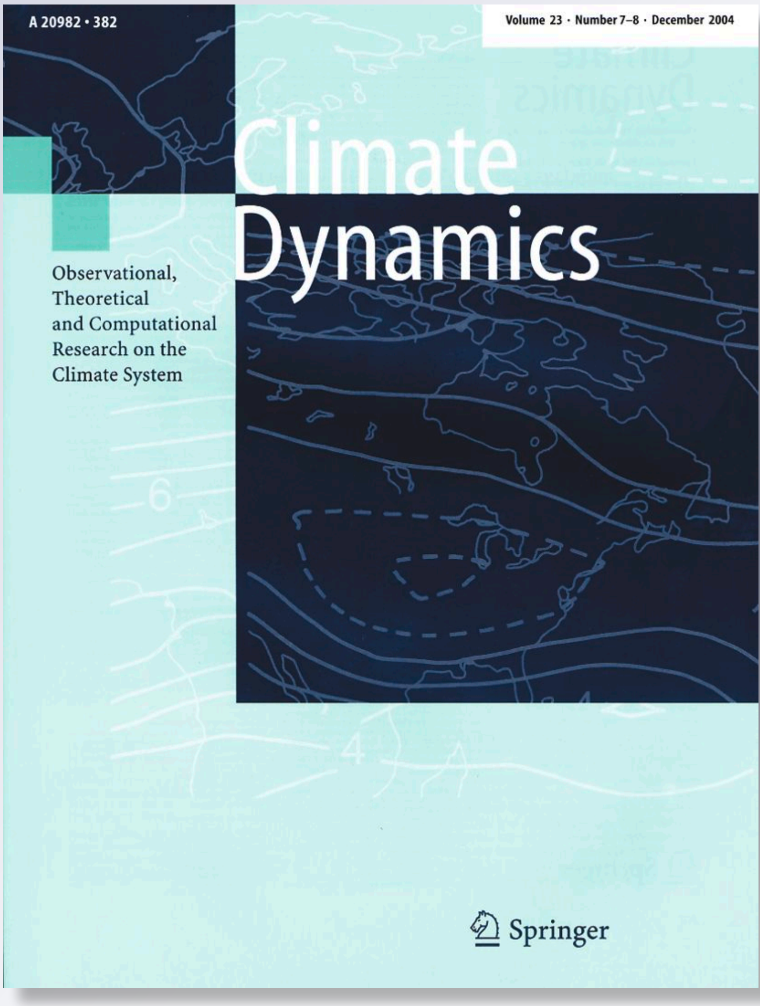

Springer

Clim Dyn (2012) 39:59–76
DOI 10.1007/s00382-011-1219-6

Evaluating uncertainties in regional climate simulations over South America at the seasonal scale

Silvina A. Solman · Natalia L. Pessacg

Received: 16 February 2011 / Accepted: 8 October 2011 / Published online: 28 October 2011

Abstract This work focuses on the evaluation of different sources of uncertainty affecting regional climate simulations over South America at the seasonal scale, using the MM5 model. The simulations cover a 3-month period for the austral spring season. Several four-member ensembles were performed in order to quantify the uncertainty due to: the internal variability; the definition of the regional model domain; the choice of physical parameterizations and the selection of physical parameters within a particular cumulus scheme. The uncertainty was measured by means of the spread among individual members of each ensemble during the integration period. Results show that the internal variability, triggered by differences in the initial conditions, represents the lowest level of uncertainty for every variable analyzed. The geographic distribution of the spread among ensemble members depends on the variable: for precipitation and temperature the largest spread is found over tropical South America while for the mean sea level pressure the largest spread is located over the southeastern Atlantic Ocean, where large synoptic-scale activity occurs. Using nudging techniques to ingest the boundary conditions reduces dramatically the internal variability. The uncertainty due to the domain choice displays a similar spatial pattern compared with the internal variability, except for the mean sea level pressure field, though its magnitude is larger all over the model domain for every variable. The largest spread among ensemble members is found for the ensemble in which different combinations of physical parameterizations are selected. The perturbed physics ensemble produces a level of uncertainty slightly larger than the internal variability. This study suggests that no matter what the source of uncertainty is, the geographical distribution of the spread among members of the ensembles is invariant, particularly for precipitation and temperature.

Keywords Regional climate modeling · South America · Uncertainty · MM5 model

Abberivations

MM5	Fifth-generation Pennsylvania-State University-NCAR non-hydrostatic mesoscale model
ERA40	European reanalyses
SA	South America
RCM	Regional climate model
GCM	General circulation model
IV	Internal variability
KF	Kain–Fritsch cumulus scheme
GR	Grell cumulus scheme
BM	Betts–Miller cumulus scheme
KF2	Updated version of Kain–Fritsch cumulus scheme
PBL	Planetary boundary layer
MRF	Medium range forecast model
ETA	ETA planetary boundary layers scheme
RMSD	Root mean square difference
slp	Sea level pressure
SST	Sea surface temperature
SACZ	South Atlantic convergence zone

S. A. Solman (✉)
Centro de Investigaciones del Mar y la Atmósfera
CIMA/CONICET-UBA, DCAO/FCEN, UMI-IFAECI/CNRS,
CIMA-Ciudad Universitaria, Pabellón II-Piso 2 (1428),
Buenos Aires, Argentina
e-mail: solman@cima.fcen.uba.ar

N. L. Pessacg
Centro Nacional Patagónico (CONICET), Puerto Madryn,
Chubut, Argentina

ITCZ Inter-tropical convergence zone
T2m 2 m temperature

1 Introduction

Regional Climate models (RCMs) have become widely used for downscaling low-resolution reanalysis or global climate simulations over different regions of the world. Their success in simulating regional climate features at finer resolution and at a relatively low computational cost, compared with simulations performed with global climate models (GCMs), has broaden their use to assess the response of the regional climate to a variety of forcings, such as increased concentration of greenhouse gases and land-use changes, among others (Nuñez et al. 2009; Déqué et al. 2007; O'Brien et al. 2010). Most of the studies are based on a single model realization representing the control climate and a single model realization representing the regional response to a given forcing, which is inherited through the boundary conditions (at the lateral boundaries or at surface). The difference between the two simulations is then evaluated as the response to the given forcing. However, in recent years, several studies have shown that regional climate simulations are affected by several sources of uncertainty (de Elía et al. 2008; Déqué et al. 2007) and the spread among different realizations should be taken into account before drawing conclusions about the significance of the regional climate responses to the external forcings. O'Brien et al. (2010) provides a very clear example of this behavior.

The sources of uncertainty in regional climate simulations can be divided in four groups: (a) the inherent uncertainty of the climate system triggered by differences in the initial conditions, referred to as internal variability (IV); (b) the uncertainty due to nesting configuration (e.g. domain size and location, relaxation technique); (c) the uncertainty due to the liberty in the RCM set up, such as the choice of physical parameterizations; and (d) the uncertainty due to the boundary forcing (driving GCM or reanalysis). Finally, for those simulations in which the response to the increase concentration of greenhouse gases is assessed, the scenario uncertainty represents an additional source (Hawkins and Sutton 2009). Though the RCMs are constrained by the lateral boundary forcing, it has been shown that they still exhibit significant IV (Lucas-Picher et al. 2008; Giorgi and Bi 2000). The IV represents the lowest level of uncertainty that cannot be reduced but should be characterized in order to evaluate to what extent the response of the regional climate to the forcing exerted through the boundaries represents a consistent signal or is shadowed by the intrinsic uncertainty in the simulated climate. On the other hand, the arbitrary choice of model configuration and model set up also introduce additional uncertainties, mainly because simulations with different model configurations (model domain, source of driving data or nesting technique) or different choices of the physical parameterizations within the RCM may give reasonable estimates of the simulated climate, being all of them equally plausible. de Elía et al. (2008) have evaluated different sources of uncertainty in a long-term simulation using a RCM over North America. They found that the levels of uncertainty arising from the liberty of choices in the definition of configuration parameters in the RCM are comparable among themselves and are larger compared with the magnitude of the uncertainty due to IV. Moreover, they conclude that every uncertainty source does not seem to be a major problem to climate downscaling. A similar conclusion was found by Lynn et al. (2009) who performed a set of simulations with different combinations of physical parameterizations to evaluate the sensitivity of simulated climate change for the 2050s.

Several recent studies have focused particularly on evaluating the magnitude of the IV in RCMs and on characterizing its spatial and temporal distribution, its dependence on the number of model realizations and on domain size (Lucas-Picher et al. 2008; Alexandru et al. 2007; de Elía et al. 2008; Caya and Biner 2004; Wu et al. 2005; Giorgi and Bi 2000 for North American domains and Vanvyve et al. 2008 for West Africa). Most of these studies recognize that the IV exhibits a seasonal cycle for most of the variables; the IV is not uniformly distributed within the model domain and the magnitude of the IV is significantly reduced for small domains. However, these studies state that the IV could be large enough to affect the interpretation of the results when the model response to a physical forcing, such as changes in land surface conditions, are evaluated as shown by Giorgi and Bi 2000 and O'Brien et al. 2010.

In recent years, a number of coordinated efforts involving the use of ensembles of RCMs over different regions of the world have led to a large amount of simulations that allowed evaluating the uncertainties in regional climate change simulations (PRUDENCE; Christensen et al. 2001 and ENSEMBLES; Hewitt 2005 for Europe; NARCCAP; Mearns et al. 2005 for North America; CLARIS-LPB; Sanchez et al. 2010 for South America; CORDEX; Giorgi et al. 2009 for Africa). These coordinated experiments have produced a set of regional climate change simulations using different RCMs nested into different global climate models for different emission scenarios. Consequently, the sources of uncertainty included were mainly due to the scenario uncertainty and the models both regional and global.

In this work we concentrate on the evaluation of uncertainties due to IV, model configuration and model physics affecting the one-way nesting approach over South America (SA) for seasonal simulations, in an attempt to have a preliminary overview of the relative importance of different sources of uncertainty inherent to the dynamical downscaling technique, their characteristic magnitude and their spatial distribution. This analysis aims to shed light on evaluating in which areas and for what variables the uncertainties are larger, or, in other words, the regional simulation may be less reliable. Up to date there are only a limited number of studies focused on evaluating the magnitude of uncertainties of regional climate simulations over South American domains, mainly concerning uncertainties due to domain choice (Rauscher et al. 2006). Though the CLARIS-LPB project is contributing to fill this gap mainly through a coordinated experiment for simulating climate change over SA, no systematic evaluation of different uncertainty sources has been performed for this region. Due to computational limitations, we concentrate on seasonal simulations (as in Alexandru et al. 2007). This first step could serve as a basis to evaluate whether climate change projections performed within the CLARIS-LPB framework are robust or fall within the intrinsic level of uncertainty.

The paper is structured as follows: Sect. 2 describes the experimental design and the metrics used for evaluation. In Sect. 3 results from the ensemble of simulations focused on different sources of uncertainty are presented. Section 4 includes a discussion about the hierarchy of sources of uncertainty evaluated. Finally, conclusions and discussion of the results are presented in Sect. 5.

2 Methodology

2.1 Brief description of the MM5 model, model domain and driving data

The model used in this study is version 3.7 of the Fifth-generation Pennsylvania-State University-NCAR non-hydrostatic Mesoscale Model (MM5) (Grell et al. 1994). Solman and Pessacg (2011) summarizes the overall model performance over SA. All the simulations in this study were performed using the explicit moisture scheme by Hsie et al. (1984). The radiation package calculates long-wave radiation through clouds and water vapor, based on Stephens (1978) and Garand (1983). Surface processes are represented by the Noah Land Surface Model (Chen and Dudhia 2001). The integration domain (Fig. 1) covers most

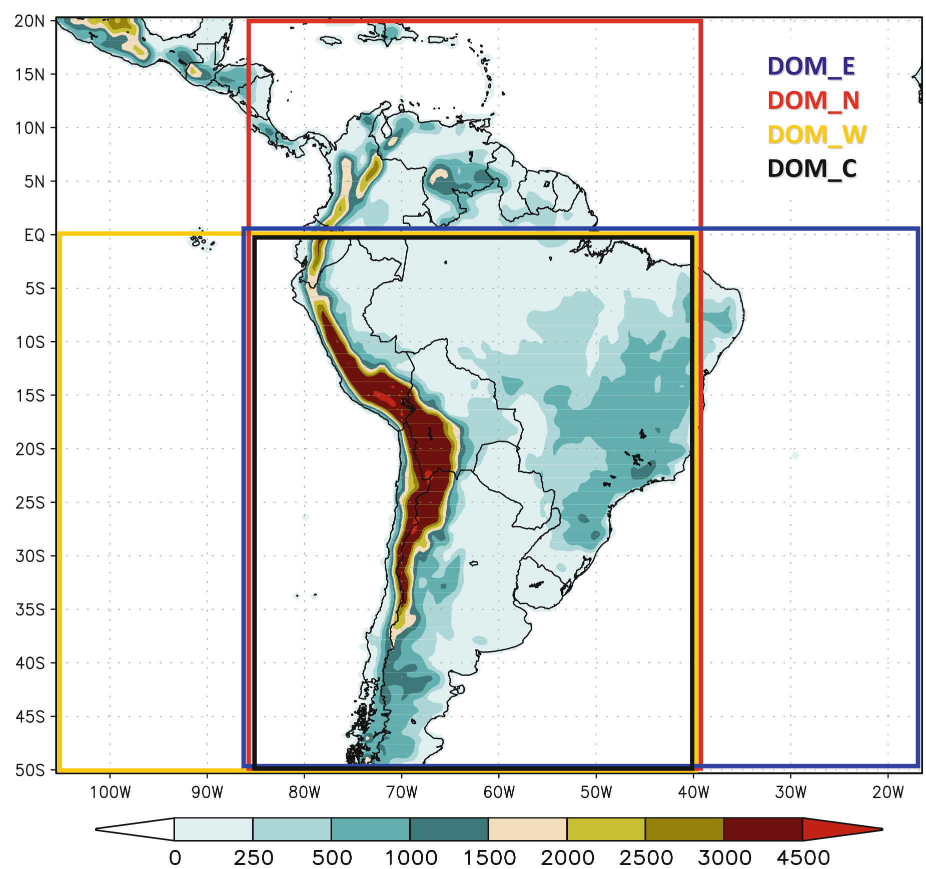

Fig. 1 Model domain and topography. The DOM_E domain is the common domain for every ensemble, except for DOM ensemble. DOM_E together with DOM_N, DOM_C and DOM_W domains define the ensemble members corresponding to the DOM ensemble. The number of grid points for DOM_E, DOM_N, DOM_W and DOM_C are 159×129; 114×177; 159×129 and 114×129, respectively

of the South American continent, from the Equator to 50°S and from 88° to 20°W with 130 points in the west–east direction and 160 points in the south–north direction for most of the experiments, except for those experiments in which the lateral boundaries were modified, as described below. It was configured on a Mercator projection grid with a resolution of roughly 50 km. In the vertical 23 sigma levels were used with the model top at 50 hPa. The land–sea mask and topography have been derived from the US Navy 10-min resolution dataset. Vegetation and soil properties were obtained from USGS vegetation/land use data base.

Initial and boundary conditions for the regional model were provided by the European Centre for Medium-range Weather and Forecasting reanalysis data set (ERA40) (Uppala et al. 2005), available at 1.125° × 1.125° resolution. Boundary conditions were updated each 6-h. Lateral boundary conditions are specified in the model over a boundary relaxation zone covering the outermost five grid points at each side, with a relaxation constant that decreases linearly away from the outermost boundaries. Sea surface temperature (SST) was also prescribed from the ERA40 dataset. The land surface model coupled to the regional model also requires additional datasets for initial conditions over land. These include soil temperature and soil moisture at four layers below the surface (0–7; 7–28; 28–100 and 100–289 cm, respectively) prescribed from the ERA40 reanalysis database.

2.2 Experimental design

All model integrations were performed for the period October 1st to December 30th 1986. This period was selected because it is characterized by contrasting conditions, with anomalous wet (dry) conditions over La Plata Basin-LPB (South Atlantic Convergence Zone-SACZ) during November and anomalous dry (wet) conditions over LPB (SACZ) during December, resembling one of the most important intraseasonal variability patterns of precipitation over SA during the warm season, the well-known see–saw pattern (Nogués-Paegle and Mo 1997).

Four groups of ensemble experiments were built based on a variety of sources of uncertainty in regional climate simulations: initial conditions; domain geometry; physical parameterizations and physical parameters using the Grell cumulus scheme (Grell 1993) as described in Table 1. It has been demonstrated that the ensemble size has an impact on the estimation of the magnitude of the uncertainty (Alexandru et al. 2007; Lucas-Picher et al. 2008). In order to produce comparable estimates of the magnitude of the uncertainty due to different sources, every ensemble was built using four ensemble members. Though the number of ensemble members could be questioned, the computational resources have been a critical issue limiting the number of simulations included in this work. In what follows the rationale behind the generation of each ensemble is presented.

The IV was evaluated by changing the starting date of the simulations. This set of simulations started with initial conditions 1 day apart, from October 1st to October 4th, 1986 and last until December 30th 1986. The ensemble is referred to as IV ensemble. In order to quantify the IV for simulations using grid nudging, we perform a second ensemble accounting for the IV, but in this case every simulation was forced within the model domain, by applying grid nudging of the winds above the planetary boundary layer (PBL). This ensemble is referred to as IV NUD ensemble. The IV and IV NUD ensembles were analyzed in order to evaluate to what extent the use of nudging techniques may be detrimental in capturing the IV in regional climate simulations. Apparently, there is no consensus in the literature about the use of nudging techniques in RCMs (Alexandru et al. 2007; Colin et al. 2010), though some preliminary analysis using the MM5 model over SA suggests that the use of nudging techniques improves model performance (Solman and Pessacg 2011).

In most of the exercises using RCMs over different regions of the world, the definition of the model domain is somewhat arbitrary, though some studies have already shown that domain choice is critical for regional climate model studies (Seth and Giorgi 1998; Alexandru et al. 2007 and de Elía et al. 2008 for North America; Seth and Rojas 2003 and Rauscher et al. 2006 for South America, among others). With this in mind, an ensemble of simulations was performed over four different domains, referred to as DOM ensemble. The definition of the domains is displayed in Fig. 1. Note that for the set of simulations corresponding to the DOM ensemble, not only the location of the boundaries varies but also the total number of grid points, being the DOM_E and DOM_W simulations comparable in terms of the number of grid points in both meridional and zonal direction, the DOM_N simulation has an increased (reduced) number of grid points in the north–south (east–west) direction and the DOM_C simulation covers a smaller domain, compared with the rest of the ensemble members.

Lessons learned from previous sensitivity studies to the choice of physical parameterizations in RCMs suggest that the uncertainty introduced by the variety in the model physics in a RCM can be quite important. Solman and Pessacg (2011) have shown that a large sensitivity to the choice of the cumulus and PBL schemes is found for seasonal scale simulations of precipitation over SA using the MM5 model. Furthermore, the choice of physical

Table 1 List of simulations performed, indicating the name of the ensemble; the starting date of each member, the model domain, the use of grid nudging technique, the combination of cumulus and PBL schemes, the parameters in the Grell cumulus scheme and the name of the experiment

ENSEMBLE	Starting date	Model domain	Grid nudging	Physics	Parameters	Name of the experiment
IV	Oct 1st 1986	East	No	KF/MRF	No	1 Oct
	Oct 2nd 1986	East	No	KF/MRF	No	2 Oct
	Oct 3rd 1986	East	No	KF/MRF	No	3 Oct
	Oct 4th 1986	East	No	KF/MRF	No	4 Oct
IV NUD	Oct 1st 1986	East	Yes	KF/MRF	No	1 Oct
	Oct 2nd 1986	East	Yes	KF/MRF	No	2 Oct
	Oct 3rd 1986	East	Yes	KF/MRF	No	3 Oct
	Oct 4th 1986	East	Yes	KF/MRF	No	4 Oct
DOM	Oct 1st 1986	East	No	KF/MRF	No	DOM_E
	Oct 1st 1986	West	No	KF/MRF	No	DOM_W
	Oct 1st 1986	North	No	KF/MRF	No	DOM_N
	Oct 1st 1986	Center	No	KF/MRF	No	DOM_C
PHYS 1	Oct 1st 1986	East	No	KF/ETA	No	KF/ETA
	Oct 1st 1986	East	No	GR/MRF	No	GR/MRF
	Oct 1st 1986	East	No	GR/ETA	No	GR/ETA
	Oct 1st 1986	East	No	BM/MRF	No	BM/MRF
PHYS 2	Oct 1st 1986	East	No	KF2/MRF	No	KF2/MRF
	Oct 1st 1986	East	No	GR/MRF	No	GR/MRF
	Oct 1st 1986	East	No	KF/MRF	No	KF/MRF
	Oct 1st 1986	East	No	BM/MRF	No	BM/MRF
PARAM	Oct 1st 1986	East	No	GR/MRF	DP = 50 hPa DT = 100 s	P1
	Oct 1st 1986	East	No	GR/MRF	DP = 150 hPa DT = 100 s	P2
	Oct 1st 1986	East	No	GR/MRF	DP = 150 hPa DT = 900 s	P3
	Oct 1st 1986	East	No	GR/MRF	DP = 50 hPa DT = 1,800 s	P4

KF, GR, BM and KF2 indicate the cumulus schemes used, respectively, Kain–Fritsch (Kain and Fritsch 1993), Grell (Grell 1993), Best–Miller (Betts and Miller 1993) and Kain Fritsch 2 (Kain 2004). MRF (Bright and Mullen 2002) and ETA (Mellor and Yamada 1974) indicate the PBL schemes used, respectively

parameterizations in a RCM is usually defined in terms of model performance, though it has been shown that no single combination of cumulus and PBL schemes is found to outperform over the entire domain and the ensemble approach arises as the best option (Solman and Pessacg 2011). Moreover, some authors suggest that using different combinations of physical parameterizations in a RCM may result in differences in the simulated climate comparable to that found when using different RCMs. de Elía et al. 2008 showed that the largest uncertainties in long-term simulations with a RCM were found using different model versions, in which several parameterizations were changed from one version to another. In order to evaluate the extent to which the choice of physical parameterizations can produce a range of estimates of the simulated climate and put this range in the context of the IV, two sets of ensembles accounting for the choice in physical parameterizations have been performed. One of them was built by changing the combination of cumulus and PBL schemes, hereafter PHYS1 ensemble. The second one was built by changing only the cumulus scheme, referred to as PHYS2 ensemble. The purpose of analyzing these two ensembles separately is to evaluate to what extent the level of uncertainty due to the choice of physical parameterizations depends on how the ensemble is built. It is important to have in mind that the combination of parameterizations of physical processes in a model is subject to some limitations due to strong interlinks among them so that not all the combinations may give realistic responses. The PHYS1 and PHYS2 ensembles have been built based on previous sensitivity studies using the MM5 model (Solman and Pessacg 2011; Fernández et al. 2007; Lynn et al. 2009; Tadross et al. 2006).

Regarding the physical parameterizations, parameter choice deserves particular attention. Certain closure parameters of the parameterized processes may be based on incomplete physical knowledge or may be tuned under specific test cases, so that their values may be somewhat arbitrary. Consequently, ensembles of simulations using ranges of plausible values for such parameters have become a suitable methodology to produce probabilistic climate predictions (Murphy et al. 2004, 2007 using a global climate model and Yang and Arrit 2002 using a RCM over North America). This so called perturbed physics ensemble has been shown to capture much of the uncertainty due to model imperfections. In this work we constructed ensemble of simulations by perturbing two parameters controlling the closure assumptions in the Grell cumulus scheme: the convective timescale (DT) and the maximum lifting depth for an unstable parcel (DP) in a similar way as described in Yang and Arrit (2002). This ensemble is referred to as PARAM ensemble.

A summary of all simulations discussed in this work is presented in Table 1.

2.3 Evaluation methods

A measure of the uncertainty for each ensemble is quantified by means of the spread among the ensemble members, using the variance estimated between each four-member ensemble, as in Alexandru et al. 2007, which will be referred to as the inter-member variance:

$$\sigma^2_{ens}(i,j,t) = \frac{1}{M}\sum_{m=1}^{M}\left[X_m(i,j,t) - \langle X\rangle(i,j,t)\right]^2 \tag{1}$$

where M is the number of ensemble members ($M = 4$ for each of the ensembles evaluated throughout this study); $X_m(i,j,t)$ represents the value of the variable X at grid point (i,j) at time t, for the individual ensemble member m. $\langle X\rangle(i,j,t)$ represents the ensemble mean, defined as:

$$\langle X\rangle(i,j,t) = \frac{1}{M}\sum_{m=1}^{M}X_m(i,j,t) \tag{2}$$

Since the inter-member variance among ensemble members varies in space and time, spatial and temporal averages of (1) have been calculated. As a measure of the spatial distribution of the spread among individual members of the ensembles, the square-root of the time-averaged inter-member variance was computed:

$$\sqrt{\overline{\sigma^2_{ens}(i,j,t)}^{t}} = \sqrt{\frac{1}{N}\sum_{t=1}^{N}\sigma^2_{ens}(i,j,t)} \tag{3}$$

where N is the number of time-steps. Since all simulations cover a 90-days period and model outputs every 6 h were saved, the number of time-steps is $N = 360$ for every ensemble, except for the IV and IV NUD ensembles in which 86 days ($N = 344$) were considered. For precipitation daily outputs were used. The spin-up period is retained in order to keep the longer available time-series. Equation 3 quantifies the climate of the spread among ensemble members. A large (small) value of this quantity indicates a large (small) discrepancy among individual members of the ensemble.

The spatially averaged time averaged standard deviation was computed as the square root of the spatially averaged and time averaged inter-member variance:

$$\sqrt{\overline{\overline{\sigma^2_{ens}(i,j,t)}^{t}}^{x,y}} = \sqrt{\frac{1}{I}\times\frac{1}{J}\times\frac{1}{N}\sum_{i=1}^{I}\sum_{j=1}^{J}\sum_{t=1}^{N}\sigma^2_{ens}(i,j,t)} \tag{4}$$

where I and J represent the number of grid points in the east–west (x) and north–south (y) directions, respectively. The five outermost grid points were excluded for calculating the spatial average. This measure summarizes the mean spread among ensemble members.

To evaluate to what extent each individual member differs with respect to the ensemble mean, the temporal evolution of the domain-averaged squared difference between each ensemble member and the ensemble mean is quantified by means of the root mean square difference (RMSD):

$$RMSD_m(t) = \sqrt{\overline{\left(X_m(i,j,t) - \langle X\rangle(i,j,t)\right)^2}^{x,y}} \tag{5}$$

This quantity allows exploring the regime dependence of the discrepancy between each individual member with respect to the ensemble mean.

Finally, in order to put the ensemble spread in the context of the natural variability of any variable, we also defined the ratio between the spread among the ensemble members and the mean temporal variability of the ensemble.

$$R(i,j) = \frac{\sqrt{\overline{\sigma^2_{ens}(i,j,t)}^{t}}}{\sqrt{\overline{\left\langle\left(X_m(i,j,t) - \overline{X_m(i,j)}^{t}\right)^2\right\rangle}^{t}}} \tag{6}$$

As discussed by Lucas-Picher et al. (2008) this ratio measures the relative importance of the ensemble spread with respect to the natural variability of the variable analyzed. Moreover, it tells to what extent the driving fields exert a control on the RCM simulation. A small ratio (R « 1) indicates that the ensemble spread is insignificant compared with the natural variability, while a ratio close to 1 or larger indicates that the driving field has limited control on the RCM and consequently the uncertainty introduced by the RCM is significantly large.

These statistics will be evaluated for precipitation, 2 m temperature and sea level pressure (slp) fields.

3 Results

3.1 Internal variability

The spatial distribution of the square root of the time-averaged inter-member variance (Eq. 3) for the IV ensemble is shown in Fig. 2a, d and g, for mean slp, temperature and precipitation fields, respectively. The first thing to note is that for every variable the IV is not uniformly distributed within the domain. For slp large values, indicating large discrepancies among individual members, are found over the southeastern Atlantic Ocean, reaching a maximum value of approximately 1.6 hPa. The western and northern boundaries of the domain are inflow boundaries; consequently, they are dominated by the driving fields making the IV very weak. The eastward propagation of synoptic systems and their characteristic paths explain the location of the maximum spread in the slp field close to the outflow boundary. The temporal variability of the slp field displayed in Fig. 2b, the denominator of Eq. 6, is characterized by maximum values at high latitudes along the storm-track and a quasi monotonic decrease towards the north. Though Fig. 2b displays the temporal variability for a particular season, the spatial distribution is similar to the temporal variability calculated over longer-term period (e.g. Jones and Simmonds 1993). However, the ratio between the inter-member spread and the temporal variability (Eq. 6) displayed in Fig. 2c tells that the IV characterizing the slp field is very low compared with the natural variability throughout the domain, reaching a maximum of 0.2 over the same area where the IV is the largest. The low values of this ratio suggest that the boundary conditions exert a dominant forcing in the RCM solution and the different solutions do not deviate much each other.

For temperature (Fig. 2d), the Amazon region is characterized by the largest values of IV ranging from 1 to 1.5°C. Over the rest of the continent, the spread among ensemble members is generally less than 1°C. Over the ocean the SST forcing limits the IV of the 2 m temperature. The temporal variability for this variable (Fig. 2e) attains large values over the subtropical latitudes, where the day to day synoptic activity is more intense, accordingly, the ratio between the inter-member standard deviation and the natural standard deviation remains low over central Argentina but reaches values of around 0.5 over the Amazon region.

The spatial distribution of the inter-member spread for precipitation (Fig. 2g) is strongly related with the spatial distribution of the precipitation itself. During the simulated period, the largest amount of precipitation is observed over tropical SA with a maximum over the South Atlantic Convergence Zone (SACZ) (see Solman and Pessacg 2011 for reference). Accordingly, the largest inter-member variability is found over that area. Note that the magnitude of the ensemble spread is larger than 4 mm/day over much of tropical SA. The temporal variability of precipitation (Fig. 2h) shows maximum values over the SACZ area, accordingly, the ratio between the inter-member spread and the temporal variability (Fig. 2i) is relatively low over SACZ and reaches large values over the Amazon region (close to 0.7), indicating that each ensemble member behaves very differently. This suggests that the domain is large enough and the RCM is able to develop independent solutions within the model domain.

Overall, the largest values of IV for temperature and precipitation are found over tropical regions, well within the model domain. Moreover, these regions display also the largest values of the ratio between the IV and the natural variability. According to Alexandru et al. (2007) who evaluated the IV at seasonal scale over North America, using less than 5 members to build the ensemble may not give a robust estimate of the magnitude of the IV. However, our results are comparable to their, in terms of the magnitude of the spread among the ensemble members for precipitation. Moreover, the limited length of the integrations could also cause an overestimation in the temporal variability, thus limiting the values of the ratios displayed in Fig. 2. Lucas-Picher et al. (2008) in their analysis of the IV over North America found ratios close to one using simulations spanning 10 years.

The temporal evolution of the RMSDs (Eq. 5) for each individual member of the ensemble, averaged over the model domain is displayed in Fig. 3 for the three variables analyzed. Besides the spin up period, in which large differences are found among the individual members of the ensemble, there are some specific events in which the simulations differ the most, particularly for the slp, suggesting that the magnitude of the IV is regime dependent. Figure 3 indicates that there is no trend in the time evolution of the RMSDs for any variable, except for the spin-up period, as expected, in agreement with Alexandru et al. (2007), but contrary to Wu et al. (2005) who showed that the impact of the initial conditions decreases as the simulation length increases. Figure 3 suggests that the magnitude of the IV can be estimated using simulations spanning only a limited number of months.

The analysis of the IV when the regional model uses nudging techniques within the model domain throughout the integration is summarized in Figs. 4 and 5. As expected, the magnitude of the spread among ensemble members is reduced, compared with results shown in Fig. 2, due to the strong control of the driving fields within the model domain. It is worth to mention that the temporal variability for every ensemble (IV NUD; DOM; PHYS and PARAM; not shown) is very similar to that of the IV ensemble both in terms of magnitude and spatial distribution, for every

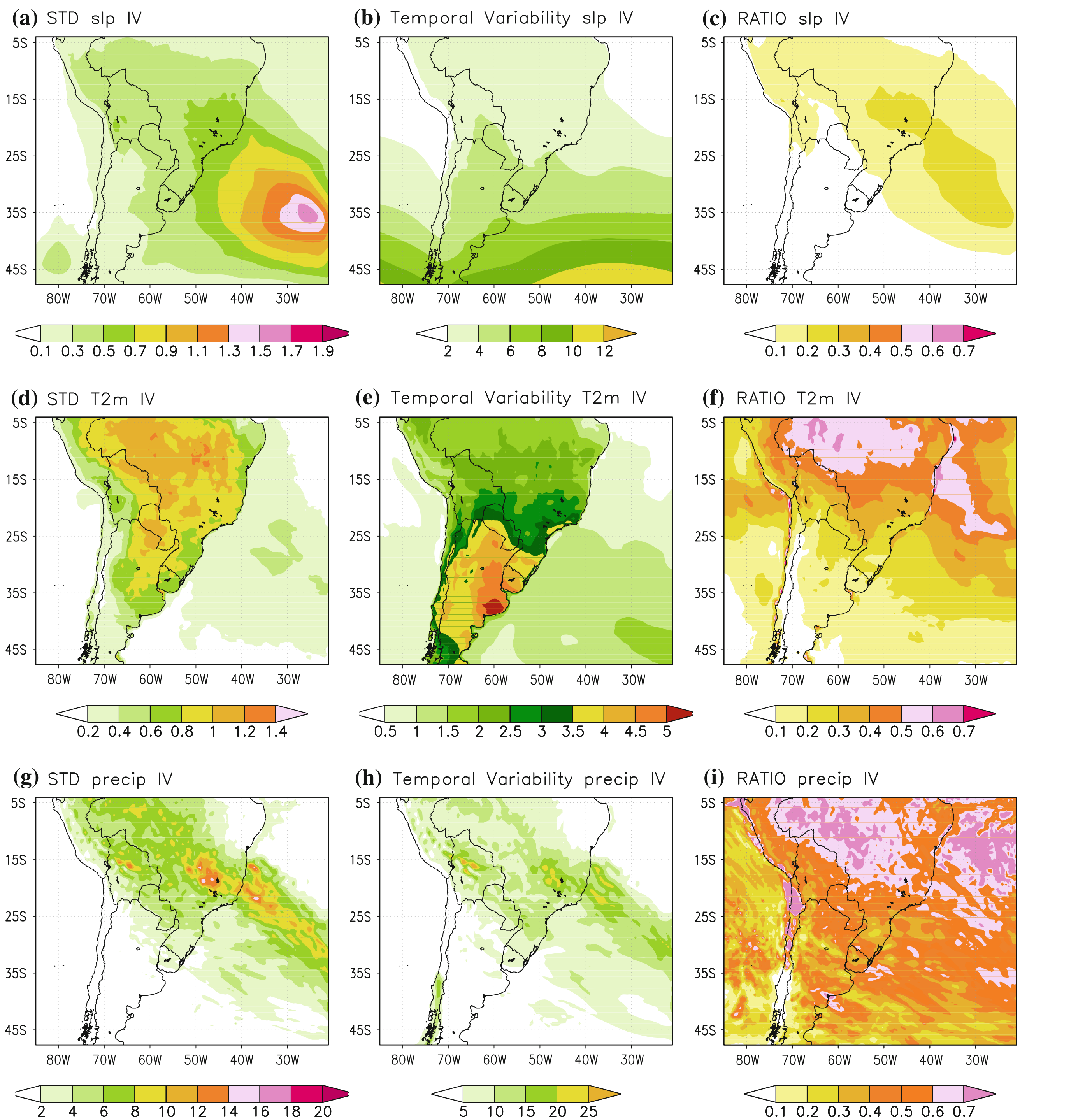

Fig. 2 Square root of the time-averaged inter-member variance for the IV ensemble for **a** slp (hPa); **d** 2 m temperature (T2 m) (°C) and **g** precipitation (mm/day). Temporal variability for the 86-days period averaged over the four ensemble members of the IV ensemble for **b** slp (hPa); **e** T2 m (°C) and **h** precipitation (mm/day). Ratio between the inter-member spread and the temporal variability for slp **c**, T2 m **f** and precipitation **(i)**

variable analyzed. The lack of freedom in the simulations using grid nudging of the winds eliminates the possibility of individual ensemble members to differ each other, reducing the ratio of IV and temporal variability to very low values, particularly for slp and temperature, and to a lesser extent for precipitation (not shown). The temporal evolution of the RMSDs for each member of the IV NUD ensemble (Fig. 5) shows that for slp the individual

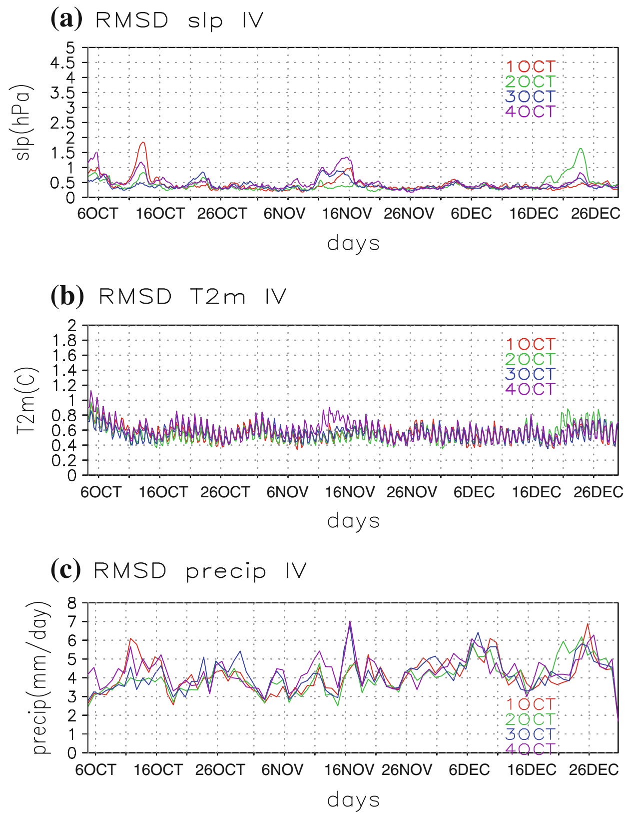

Fig. 3 Temporal evolution of the RMSDs averaged over the model domain for the IV ensemble for **a** slp (hPa); **b** T2 m (°C) and **c** precipitation (mm/day)

members are very close each other and no dependence on the regime is evident, in contrast with results from the IV ensemble, except for the spin-up period. For temperature and precipitation, the RMSDs are also reduced compared with the IV ensemble, but, oscillate around 0, 3°C and 2 mm/day, respectively. These results question the convenience of using nudging techniques for climate studies, moreover, for evaluating to what extent the response to any external forcing can be considered as significantly different from noise. Underestimating the IV using nudging techniques may lead to erroneous evaluation of the signal to noise ratio.

3.2 Uncertainty due to Domain choice

Figures 6 and 7 summarize the DOM ensemble results, where the comparison is made only for the common domain (see Fig. 1). It is interesting to note that the magnitude of the inter-domain variability for the slp (Fig. 6a) is several times larger than the magnitude of the IV all over the domain (Fig. 2a). Moreover, the spatial distribution of the spread among members is quite different compared with that of the IV ensemble. Larger values are found

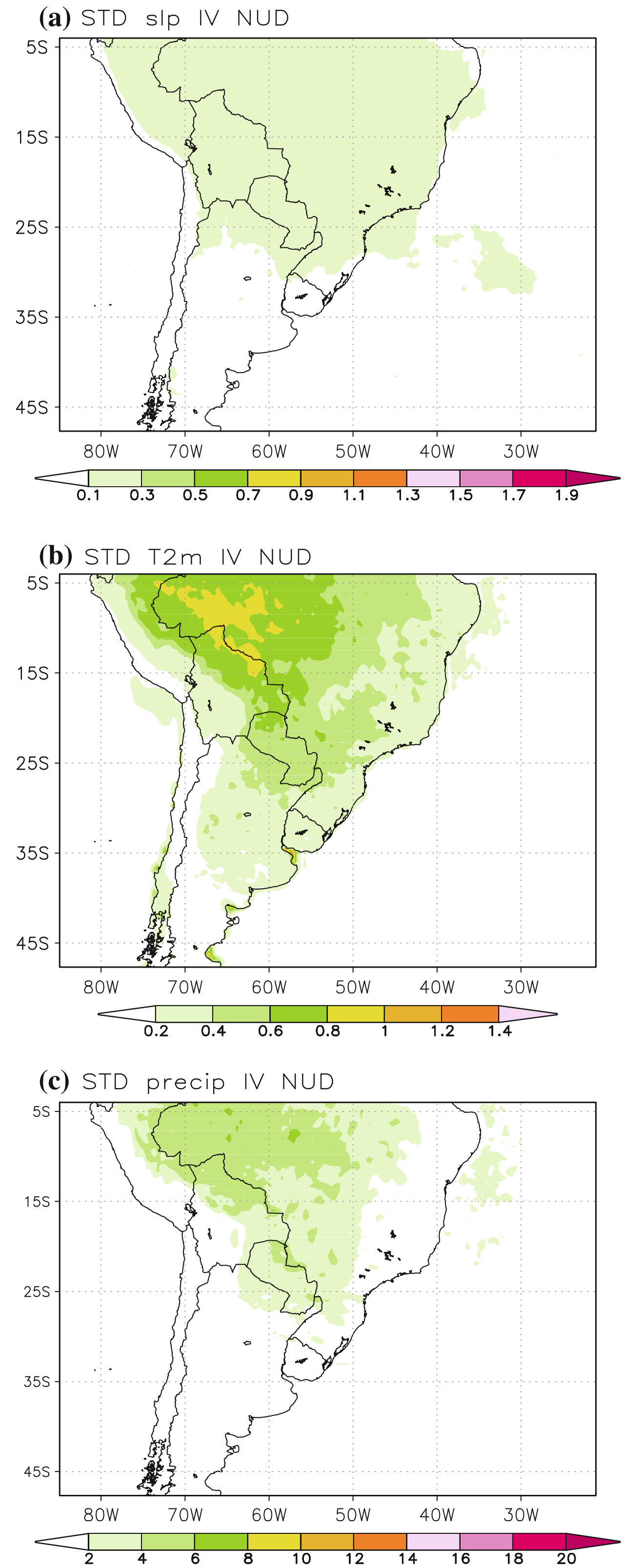

Fig. 4 Square root of the time-averaged inter-member variance for the IV NUD ensemble for **a** slp (hPa); **b** T2 m (°C) and **c** precipitation (mm/day)

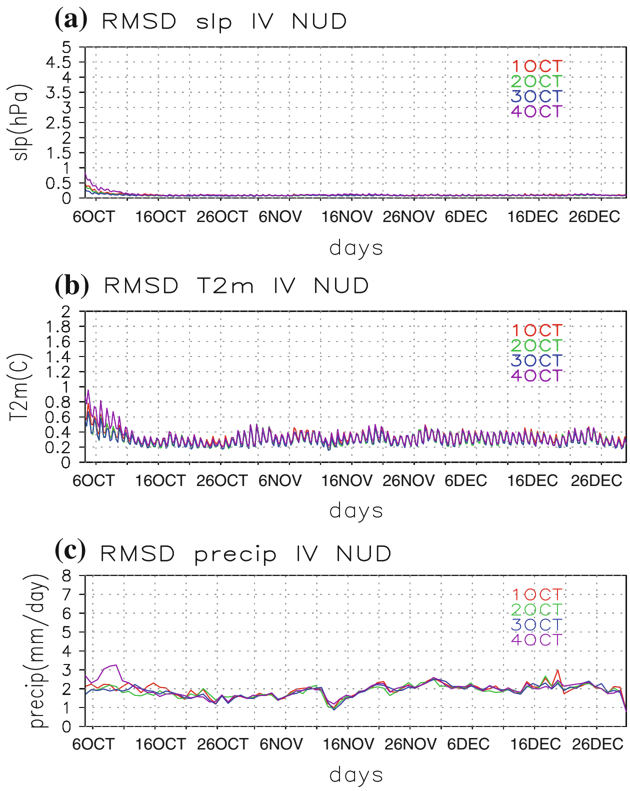

Fig. 5 Same as Fig. 3 but for the IV NUD ensemble

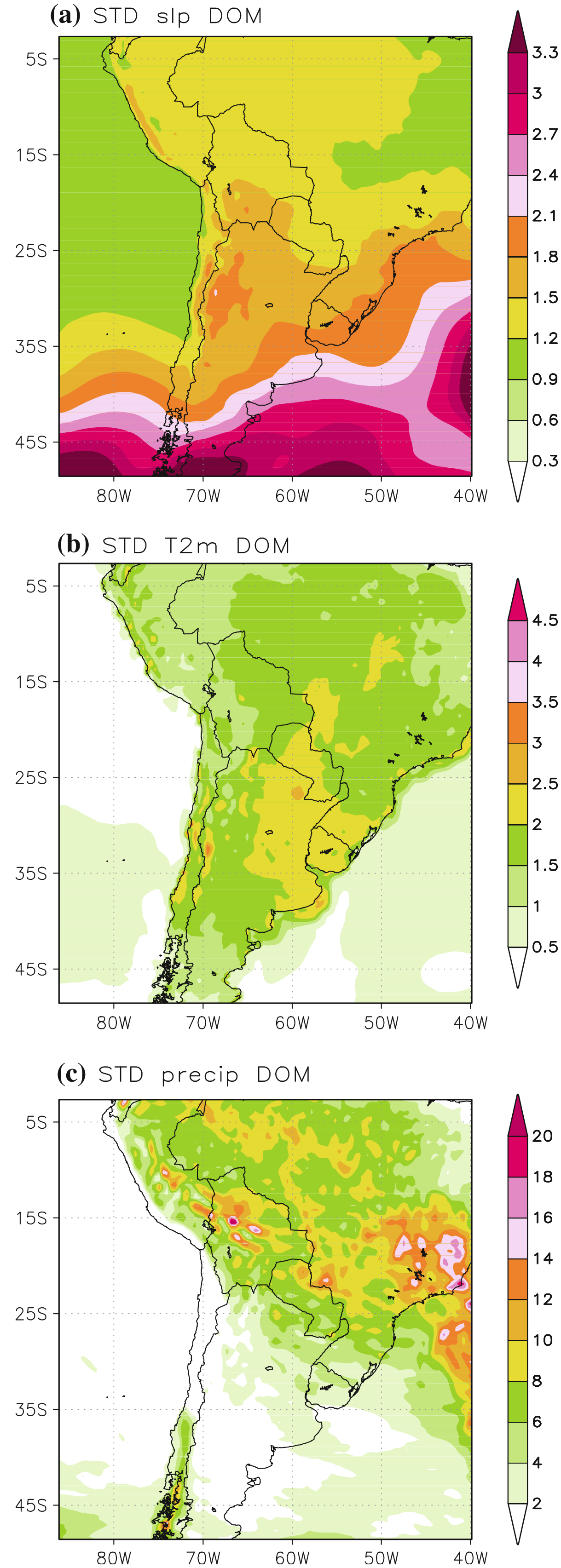

Fig. 6 Same as Fig. 4 but for the DOM ensemble

mainly at mid-latitudes, south of 35°S, particularly near the southern boundary. However, the ratio between the spread among members and the temporal variability remains smaller than 0.5 over most of the domain except over the northern and western boundaries where it is close to 0.7 and 0.8, respectively (not shown). Inspection of Fig. 7a suggests that the DOM_W simulation contributes the most to the large spread within the DOM ensemble. Moving the western boundary towards the west implies that the regional model is able to solve the evolution of synoptic systems that develop over the Pacific Ocean reaching the South American continent, conversely, for the other ensemble members the features of the synoptic systems evolving over the Pacific Ocean are given by the ERA40. Consequently the timing, intensity and location of these systems can be different from that of the driving fields, explaining the large spread over that area, where the synoptic-scale activity is more active (see Fig. 2b). Inspection of individual synoptic events highlights the different behavior of the DOM_W at a daily basis compared with the other members, which develops deeper systems evolving eastwards in the DOM_W member at higher latitudes. Every ensemble member share the same western boundary except the DOM_W experiment, suggesting that the location of the western boundary results in the largest uncertainty concerning domain choice.

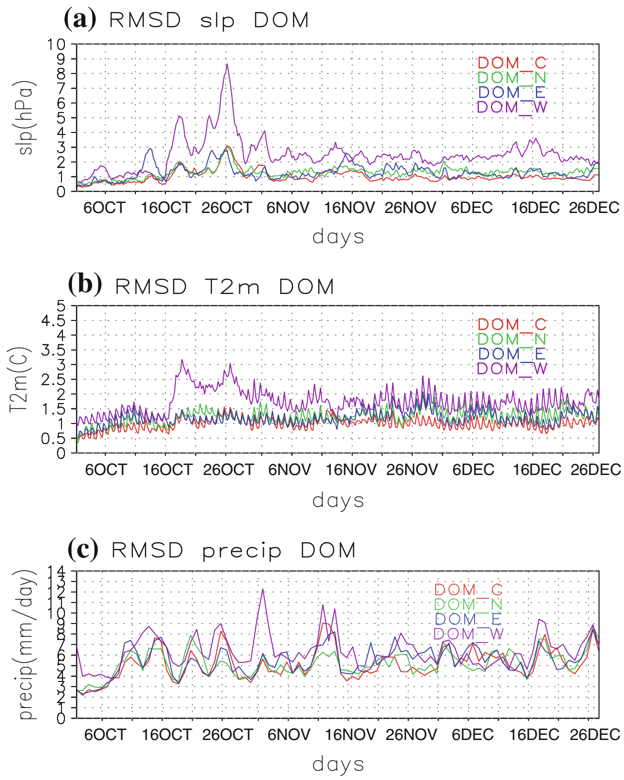

Fig. 7 Same as Fig. 3 but for the DOM ensemble

The inter-domain variability for temperature (Fig. 6b) is also larger than the IV, with the largest values over northeastern Argentina (around 2°C). However, the ratio between the inter-domain variability and the temporal variability (not shown) maintains the same spatial distribution compared with that of the IV ensemble and remains below 1.0 all over the common domain. As for the slp, the temporal evolution of the RMSD for each ensemble member (Fig. 7b) shows that the DOM_W simulation displays the largest differences with respect to the DOM ensemble, being the rest of the ensemble members quite close each other.

For precipitation the spatial distribution of the inter-domain variability (Fig. 6c) maintains a similar spatial structure compared with that of IV but its magnitude is larger, as for the slp and temperature. The ratio between the inter-domain variability and the temporal variability is also larger, with values close to 0.8 over most of tropical SA (not shown), suggesting that the uncertainty due to the choice of the location of the domain is also quite important. The temporal evolution of the RMSDs for individual members (Fig. 7c) shows that for precipitation the spread among each individual member is similar with no individual member behaving particularly different from the others. It is interesting to note that in the DOM ensemble every ensemble member has a similar domain size except the DOM_C simulation which has a smaller domain. Interestingly, the RMSDs for each individual ensemble member have similar magnitude. Some authors suggest that larger domains may lead to larger uncertainties (Alexandru et al. 2007; Lucas-Picher et al. 2008) as the regional model can deviate more from the driving fields. In our results, it is not evident that the smaller domain has any particular behavior compared with larger domains. However, it is also evident that we are not evaluating the IV for different domain sizes, but the inter-domain variability that takes into account not only different locations of the lateral boundaries but also different domain sizes.

3.3 Uncertainty due to Model Physics

The inter-member variability for the PHYS1 ensemble is displayed in Fig. 8. The spatial pattern of the inter-member variability is similar to that of the IV ensemble for slp (Fig. 2a), though the magnitude is twice as large. Accordingly, the ratio between the inter-member variability and the temporal variability increases but it still remains below 1.0, reaching maximum values of 0.6 over the subtropical western Atlantic Ocean (not shown). The temporal evolution of the RMSDs for each individual member depicts a particular behavior (Fig. 9a). It is evident that two pairs of experiments can be identified behaving differently, depending mainly on which PBL scheme is being used.

For temperature the inter-member variability (Fig. 8b) also shows a spatial pattern similar to that of the IV ensemble, but the magnitude is larger than 2.5°C all over the continental areas with values above 3°C over central Argentina and central Brazil. This may be due to one of the simulations being too warm yielding large values of inter-member spread. The temporal evolution of the RMSDs for each member, shown in Fig. 9b, clarifies this behavior. The BM/MRF experiment shows the largest differences, larger than 3°C on average, compared with the rest of the ensemble members. This experiment strongly overestimates the 2 m temperature over tropical areas, yielding large differences averaged all over the model domain, with respect to the other ensemble members. The ratio between the inter-member variability and the temporal variability (not shown) reaches values of around 0.9 over much of tropical regions. This suggests that the choice of physical parameterizations has a strong control on the simulated climate, similar to the control exerted by the driving fields.

For precipitation, the spatial distribution of the inter-member variability of the PHYS1 ensemble (Fig. 8c) is quite different compared with that of the IV ensemble. The largest values are found over northern Argentina, the Andes and over the coastal area of the SACZ. Beside this, the magnitude of the spread is larger compared with that of the IV ensemble, as expected, due to the strong impact of

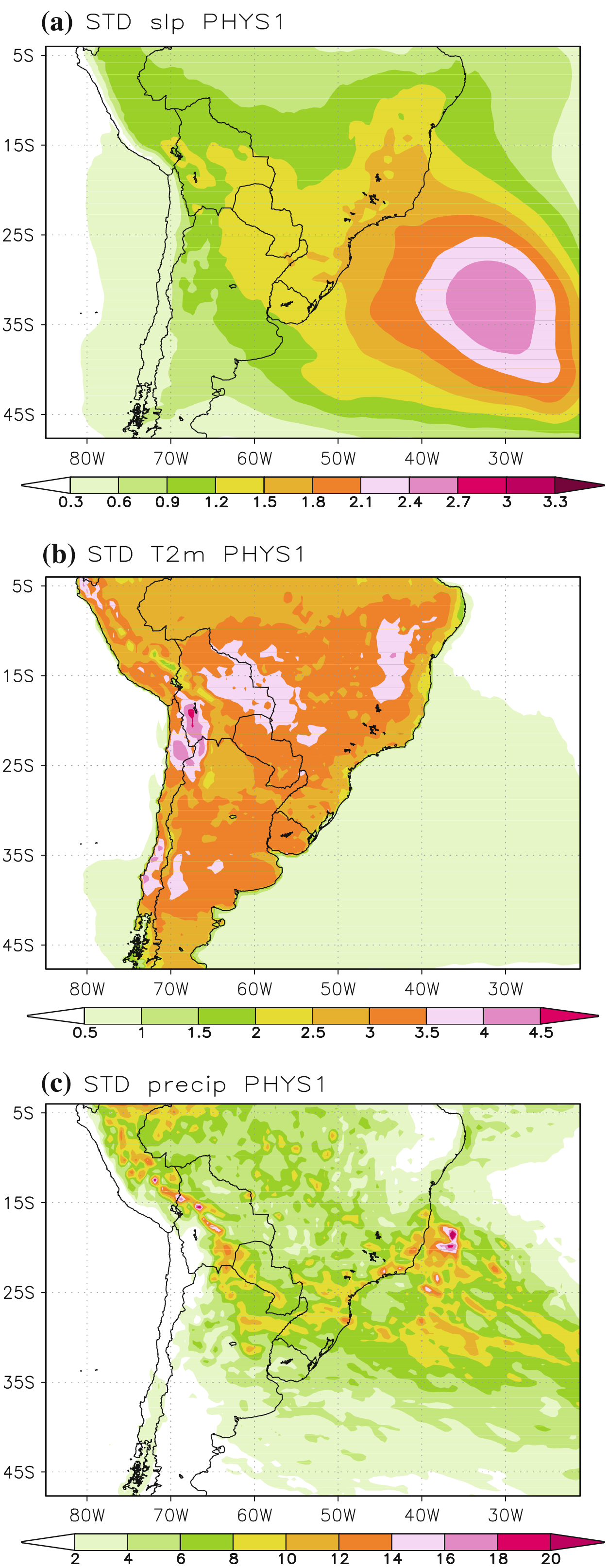

Fig. 8 Same as Fig. 4 but for the PHYS1 ensemble

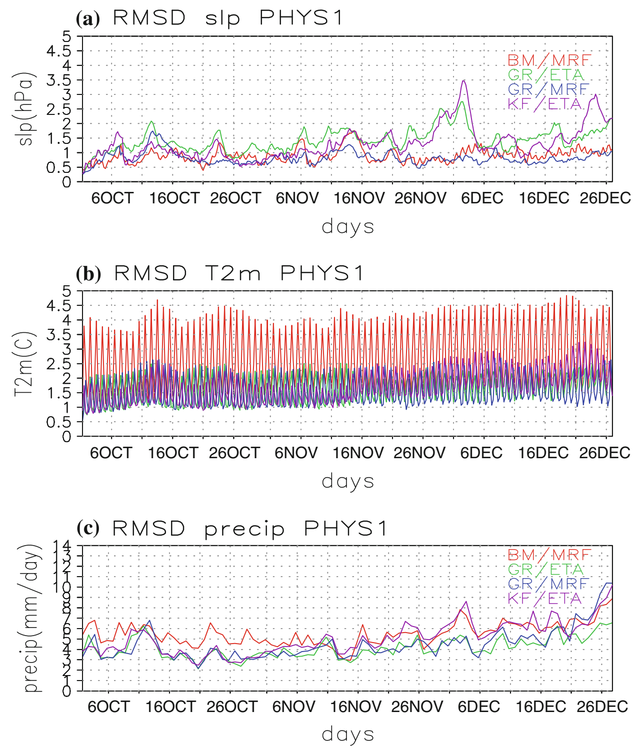

Fig. 9 Same as Fig. 3 but for the PHYS1 ensemble

both the cumulus and PBL schemes on precipitation, as shown in Solman and Pessacg (2011), yielding a ratio of inter-member variability over the temporal variability larger than 0.8 over much of the continental domain (not shown). The temporal evolution of the RMSDs shown in Fig. 9c, summarizes the particular behavior of each ensemble member. In particular, the BM/MRF, which strongly underestimates precipitation over tropical regions, arises as the member that deviates the most throughout the integration period with respect to the ensemble mean. The systematic overestimation of precipitation in the KF/ETA simulation over tropical areas of the domain (as shown in Solman and Pessacg 2011) also explains the large values of RMSD for the KF/ETA ensemble member. Fig. 9c also shows that the RMSDs seem to increase throughout the integration period, in contrast with results shown for other sources of uncertainty (see Figs. 8c and 4c). The integration period is characterized by anomalous wet conditions over SACZ during December, thus the largest differences are more evident during December when the largest precipitation events occur.

For the PHYS2 ensemble, the inter-member variability for the slp is very similar to that of the PHYS1 ensemble (Fig. 10a). For temperature Fig. 10b presents a similar spatial pattern to that of the IV and PHYS1 ensembles, with

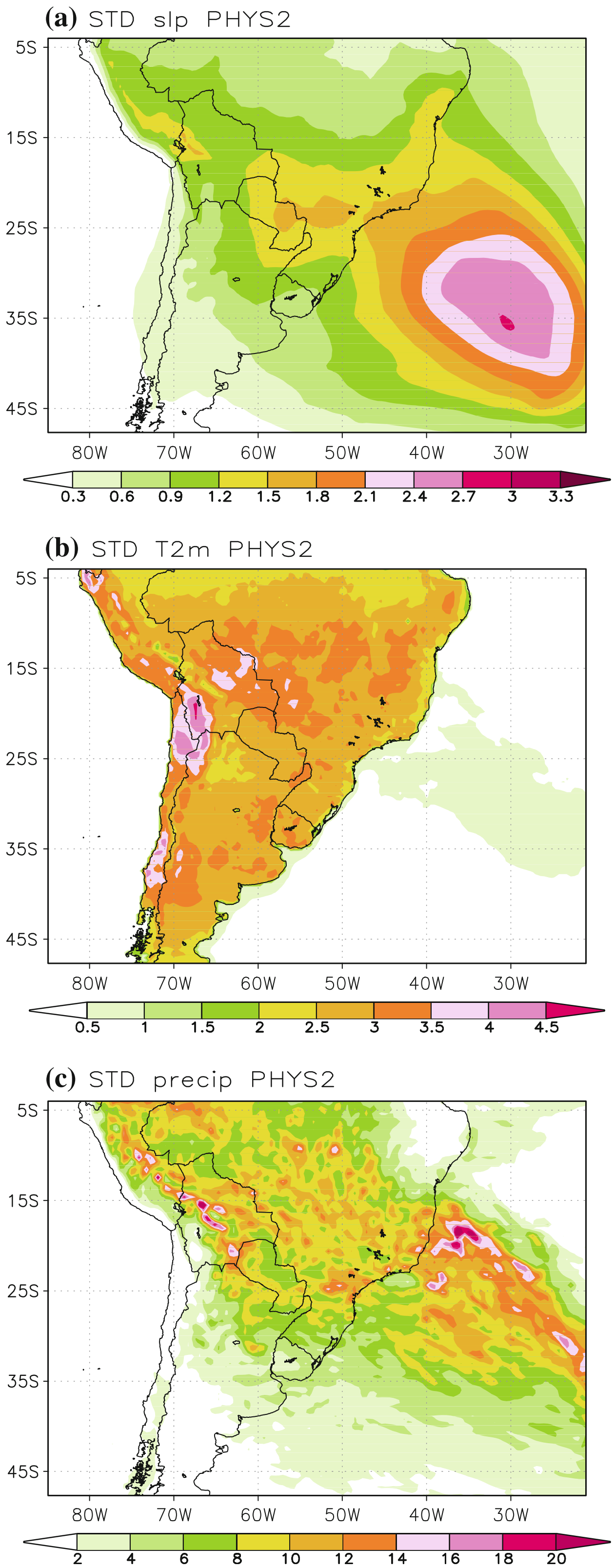

Fig. 10 Same as Fig. 4 but for the PHYS2 ensemble

values above 2.5°C over much of the continental area. However, compared with the PHYS1 ensemble, the magnitude of the ensemble spread is lower. For precipitation the inter-member variability (Fig. 10c) has a spatial distribution quite similar to that of the IV ensemble but with larger values particularly over tropical regions. Comparing the PHYS1 and PHYS2 ensembles, it is evident that the spatial pattern of the inter-member variability and its magnitude depend on how the ensemble is built. Overall, changing only the cumulus schemes, as for the PHYS2 ensemble, or changing the combination of both the cumulus and the PBL schemes, as for the PHYS1 ensemble, yields comparable estimates of uncertainty due to the choice of physical parameterizations for slp but not for temperature and precipitation. This result suggests that estimating the uncertainty due to model physics should include a broad range of possible combinations of physical schemes in order to have a robust estimation of this source of uncertainty.

3.4 Uncertainty due model physics II: Physical parameters

The inter-member spread for slp is almost the same as for the IV ensemble both in terms of spatial distribution and magnitude (Fig. 11a). Figure 11b shows that the inter-member spread for temperature is also similar to the IV ensemble, though the magnitude is slightly larger. For precipitation (Fig. 11c), the spatial distribution of the inter-member variability is similar to that of the IV ensemble, though larger values are found over the oceanic extension of the SACZ. This difference may be due to the IV ensemble uses the Kain–Fristch cumulus scheme whereas the PARAM ensemble in based on the Grell cumulus scheme. Solman and Pessacg (2011) found that the Grell (Kain–Fristch) scheme systematically underestimates (overestimates) precipitation over tropical regions, consequently, the uncertainty over tropical SA using the Grell scheme may be also underestimated compared with the ensemble using the Kan–Fristch scheme. The ratio between the inter-member variability and the temporal variability presents a similar pattern to that of the IV ensemble both in terms of the spatial distribution and magnitude. Again, the tropical regions seem to be more controlled by the specific configuration of the regional model than by the driving fields.

4 Discussion of the hierarchy of uncertainty sources

In order to summarize the relative relevance of the set of uncertainty sources evaluated in this work, Fig. 12 shows

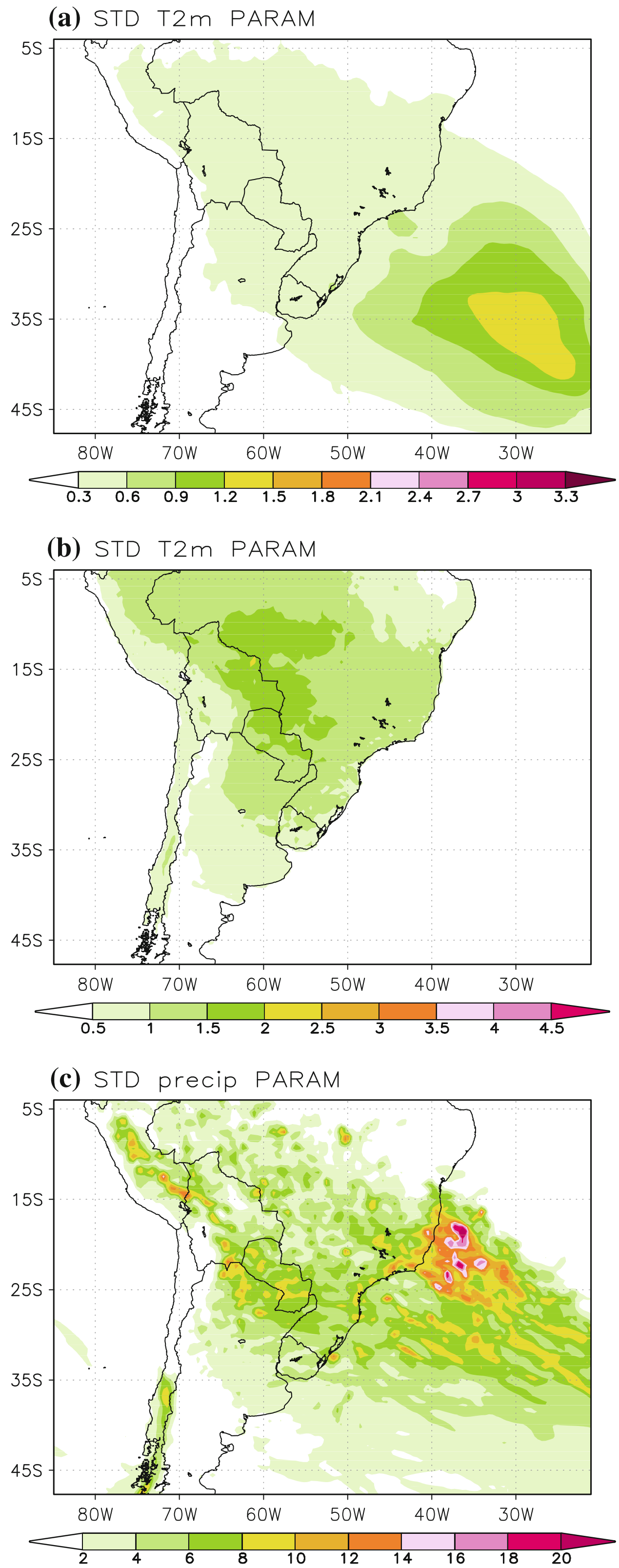

Fig. 11 Same as Fig. 4 but for the PARAM ensemble

the square root of the domain averaged time averaged inter-member variance (Eq. 4) for each ensemble for the three variables analyzed: slp, temperature and precipitation. We ordered the set of ensembles with increasing inter-member spread for temperature in a similar way as in de Elia et al. (2008), with the aim of assessing a ranking among different sources of uncertainty, and the same order has been kept for displaying the mean spread for precipitation and slp, though the ranking of the uncertainty sources is not the same. In addition, the domain averaged temporal variability (denominator of Eq. 6) for each variable is also displayed for each ensemble.

For every variable analyzed the uncertainty introduced by the initial conditions represents the lowest level of uncertainty, a noise level against which any signal regarding the response of the regional climate to any forcing, should be compared. The use of nudging techniques reduces the IV in the regional simulation. For temperature, this uncertainty source ranges from 0.3 to 0.6°C for the IV NUD and IV ensembles, respectively, whereas for precipitation, it ranges from 2 mm/day to less than 4 mm/days, respectively. Note that the magnitude of the IV is close to the estimations shown in Alexandru et al. (2007), though the number of ensemble members in this work is smaller. The uncertainty introduced by the freedom of choice in physical parameters (PARAM) seems to be comparable or slightly larger to that introduced by the initial conditions, suggesting that the impact of model imperfections is well within the characteristic noise level of regional simulations. The uncertainty introduced by the choice in the definition of the domain follows in the ranking for both temperature and precipitation, with magnitudes of approximately 1.3°C and 5.5 mm/day, respectively, but it is certainly the largest source of uncertainty for slp. This result suggests that the modeled climate depends strongly on the definition of the domain, consequently, any intercomparison exercise using different RCMs for evaluating the uncertainty in regional climate change scenarios for the near future, in which the temperature is projected to increase no more than 1°C over much of the South American continent (Marengo et al. 2010) should be performed at least using the same domain due to the large dependence of the simulated climate on domain definition. The choice of physical parameterizations represents the largest source of uncertainty for temperature, with values close to 2°C and for precipitation, in agreement with de Elía et al. (2008), though its impact on simulating slp is not so relevant (close to 1 hPa). The magnitude of the level of uncertainty due to the choice of model physics depends strongly on how the ensemble is

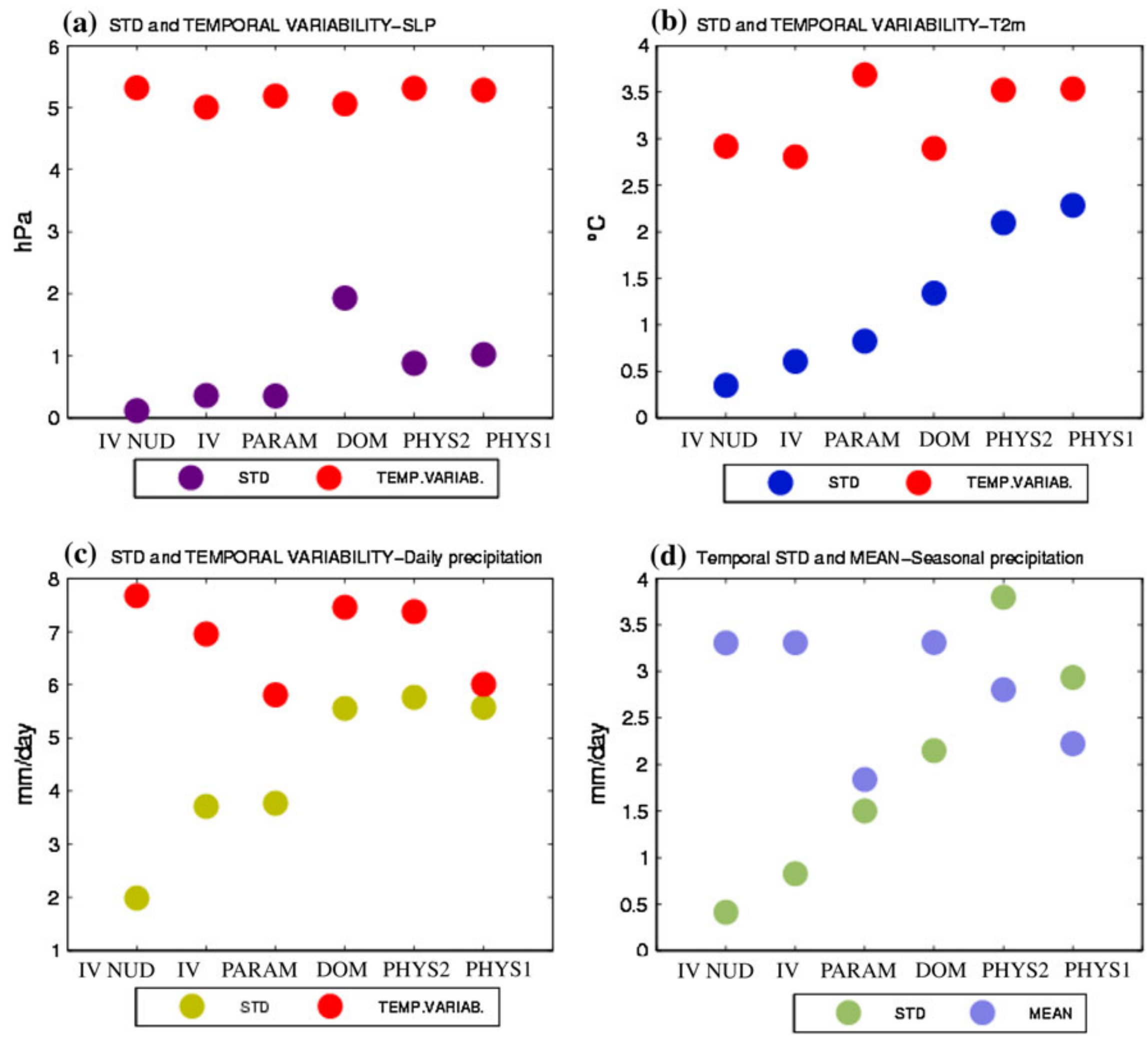

Fig. 12 Square root of the domain averaged-time averaged inter-member variance (STD) and temporal variability (*red circles*) for **a** slp (hPa), **b** T2 m (°C) and **c** precipitation (mm/day) for the set of sources of uncertainty evaluated: Internal Variability (IV); Internal Variability using grid nudging (IV NUD); physical parameters (PARAM); domain choice (DOM) and physical parameterizations (PHYS1 and PHYS2). **d** shows the domain averaged inter-member spread calculated for the seasonal average precipitation (*green circles*) and the domain average-time average precipitation (*purple circles*) for each ensemble

built, mainly for precipitation, ranging from 4.5 mm/day for the PHYS1 ensemble to 5.8 mm/day for the PHYS2 ensemble. The limited number of members in these ensembles may produce uncertainty estimates not sufficiently robust. In order to evaluate this possibility, a 6-member ensemble was built using the experiments included in PHYS1 and PHYS2, yielding values of inter-member spread of 1.1 hPa, 2.1°C and 5.6 mm/day for slp, temperature and precipitation, respectively. The magnitude of the uncertainty for slp and temperature is similar to those for the PHYS1 and PHYS2 ensembles, but not for precipitation. This suggests that large ensembles should be considered to have a robust estimate of the spread of regional climate simulations due to the freedom in the choice of physical parameterizations. This estimation could also be done building multi model ensembles that are expected to show a range of modeled climates within the same range as those obtained with the same model with different physical options.

Note that for all these sources of uncertainty the inter-member spread is always smaller compared with the temporal variability, indicating that the inter-member agreement with each other is high compared with the natural variability, in other words, the inter-member spread is not significant.

Several authors have raised the question concerning to what extent these sources of uncertainty impact on the seasonal averages. Though the sources of uncertainty are numerous, the IV has received considerable attention in the literature. de Elía et al. (2008), Alexandru et al. (2007) and

Lucas-Picher et al. (2008) agree on that the IV has an impact on seasonal averages; the longer the averaging period the smaller the impact of the IV on seasonal averages. In general we are mostly interested on the statistics of the simulated climate, rather than on the particular temporal behavior within a particular period, so the relevance of the inter-member variability on the seasonal mean is relevant. Fig. 12 includes the domain averaged inter-member spread calculated for the seasonal averages, together with the temporal and domain averaged values of precipitation (Fig. 12d). It is evident that the inter-member spread for the seasonal mean is reduced compared with the temporal mean of the inter-member spread for every ensemble, in agreement with previous studies. It is also evident that the coefficient of variation, the ratio between the inter-member spread calculated on the seasonal mean and the mean precipitation, is less than 25% for the IV ensembles, but it increases up to 60% for the DOM ensemble and a much higher value is found for the perturbed physics ensemble (PARAM ensemble). The level of uncertainty when different combinations of physical schemes are considered is even larger than the mean precipitation, yielding coefficients of variations larger than 100%, indicating that the uncertainty at the seasonal scale is important to be considered.

All the uncertainty estimates discussed above are based on simulations spanning over a single season. It has been shown that the level of uncertainty is regime-dependent. The simulated period, characterized by alternating wet and dry conditions over subtropical and tropical SA, respectively, allows including different regimes, so the results presented in this work may be representative, at least, for the austral spring season.

5 Concluding remarks

The purpose of this work is to evaluate different sources of uncertainty inherent to the regional climate modeling approach over SA with the aim of analyzing how they impact on the simulated climate. The main objective was to characterize the spatial pattern and magnitude of the uncertainty. To fulfill this aim several 4-member ensembles were performed in order to quantify the level of uncertainty due to the IV, the freedom in the domain choice, the freedom in the selection of physical parameters within a physical parameterization and the freedom in the selection of the combination of physical schemes in the regional model. The simulations were performed with the MM5 model spanning over one spring season over SA. Every simulation was driven by the ERA-40 reanalyses. For each ensemble, the ensemble spread was evaluated in terms of the square root of the variance of each individual member with respect to the ensemble mean during the integration period.

The first source of uncertainty evaluated was that arising from initial conditions, referred to as the IV. The IV is not uniformly distributed within the model domain but displays preferential regions where the IV is particularly large. For the sea level pressure, the maximum values of IV are found over the southeastern Atlantic Ocean (up to 1.7 hPa), close to the outflow boundary. For temperature, the areas with larger IV are located over tropical SA and northern Argentina with values up to 1.5°C. For precipitation the largest spread among members is found over the areas where large convective precipitation occurs, the SACZ region and tropical SA, with an inter-member spread up to 10 mm/day. As for temperature, the larger values of the inter-member spread normalized with respect to the temporal variability are confined over tropical areas, suggesting a higher control of the driving fields over mid-latitudes, as expected. Inspection of the temporal evolution of the spread among individual members suggests that the IV is regime dependent, particularly for slp and precipitation, in agreement with previous studies. Using nudging techniques reduces dramatically the IV in the regional simulation due to the strong control of the driving fields within the model domain, which inhibits the ensemble members to deviate from each other. However, it is interesting to note that the temporal variability is not affected by the use of nudging techniques for any of the variable analyzed.

The domain choice introduces a large uncertainty in the simulated fields, particularly for the slp, characterized by a large spread over the region depicting the largest eddy activity at mid-latitudes. Inspection of results reveals that moving the western boundary further to the west has a strong impact on the simulated climate. When the model domain includes a broad region upstream SA, the behavior of the synoptic-scale systems can be quite different from that of the low resolution driving fields, in terms of their intensity and location and the simulation becomes uncorrelated with the other ensemble members in which the western boundary (inflow) is closer to the South American continent. The large inter-domain variability suggests that the definition of the regional domain should include a very detailed analysis of what are the relevant mechanisms that are worth to be solved with high resolution and that could impact the variables of interest.

The spatial pattern of the ensemble spread is invariant with respect to the source of uncertainty, particularly for precipitation and temperature and, to a lesser extent, for slp. In other words, the growing error maintains a preferential direction of growth independent of the uncertainty source, though the magnitude of the uncertainty depends on the source. This allows establishing a ranking regarding the relative importance among different sources of uncertainty. The IV represents the lower level of uncertainty for every variable analyzed, in agreement with de Elía et al. (2007). The uncertainty due to the choice of model physics arises as the most important uncertainty, particularly for temperature and precipitation, with values of spread around 2°C and 5.8 mm/day, respectively. It is interesting to note that the uncertainty due to domain choice lies in between the IV and the uncertainty due to the model itself for temperature and precipitation. This result does not agree with those presented by (de Elía et al. 2008) probably due to their simulations were constrained by the use of large-scale nudging, which limits the sensitivity of the simulated climate to domain issues (Miguez-Macho et al. 2005).

Though the magnitude of the spread among members of the different set of ensembles may be quite large, it is important to remark that no matter which uncertainty source is being evaluated, the spread is generally weaker when it is compared with the natural variability, yielding ratios between the inter-member spread and the natural variability smaller than 1, suggesting that these uncertainties can be considered not significant (Rinke et al. 2006). This may be due to the day to day variability is large enough to reduce the relative importance of the uncertainty. However, when the seasonal mean precipitation is evaluated, though the magnitude of the uncertainty is weaker for every source, as in previous studies, the uncertainty due to the choice of physical parameterizations is larger than the simulated precipitation itself. The small size of our ensembles and the fact that only one season statistics is being considered may be insufficient to draw robust conclusions about the magnitude of the spread at the seasonal scale level.

This work represents an attempt to characterize uncertainties in regional climate simulations over South America; however, we must be careful in generalizing the conclusions drawn from this study using a specific RCM, a limited number of ensemble members and a limited length of the simulations. It is expected that longer simulations and larger ensembles could be performed in order to have a robust estimate of the uncertainties that will allow drawing conclusions about how reliable may be the regional climate simulations over SA.

Acknowledgments The research leading to these results has received funding from the European Community's Seventh Framework Programme (FP7/2007-2013) under Grant Agreement No 212492 (CLARIS LPB—A Europe-South America Network for Climate Change Assessment and Impact Studies in La Plata Basin). This work has also been supported by FONCYT Grant PICT05 32194, UBACyT Grant X160, Conicet Grant PIP 112-200801-00195. The authors wish to thank the comments of two anonymous reviewers for insightful suggestions that greatly helped to improve this manuscript.

References

Alexandru A, de Elia R, Laprise R (2007) Interanual variability in regional climate downscaling at the seasonal scale. Mon Weather Rev 135:3221–3238

Betts AK, Miller MJ (1993) The best Miller scheme. The representation of cumulus convection in numerical models of the atmosphere. In: Emanuel KA, Raymond DJ (eds) Amer Met Soc

Bright D, Mullen S (2002) The sensitivity of the numerical simulation of the southwest monsoon boundary layer to the choice of PBL turbulence parameterization in MM5. Weather Forecast 17:99–114

Caya D, Biner S (2004) Internal variability of RCM simulations over an annual cycle. Clim Dyn 22:33–46

Chen F, Dudhia J (2001) Coupling and advanced land surface hydrology model with the Penn State-NCAR MM5 modeling system. Part I: model implementation and sensitivity. Mon Weather Rev 129:569–585

Christensen OB, Gaertner MA, Prego JA, Polcher J (2001) Internal variability of regional climate models. Clim Dyn 17:875–887

Colin J, Deque M, Radu R, Somot S (2010) Sensitivity study of heavy precipitation in limited area model climate simulations: influence of the size of the domain and the use of the spectral nudging technique. Tellus 62A:591–604

de Elía R, Laprise R, Denis B et al (2008) Evaluation of uncertainties in the CRCM-simulated North American climate. Clim Dyn 30:113–132

Déqué M, Rowell DP, Luthi D, Giorgi F, Christensen JH, Rockel B, Jacobson D, Kjellstrom E, de Castro M, van der Hurk B (2007) An intercomparison of regional climatic simulations for Europe: assessing uncertainties in model projections. Clim Change 81:53–70

Fernández J, Montávez JP, Sáenz J, González-Rouco JF, Zorita E (2007) Sensitivity of the MM5 mesoscale model to physical parameterizations for regional climate studies: annual cycle. J Geophys Res 112:D04101. doi:10.1029/2005JD00664

Garand L (1983) Some improvements and complements to the infrared emissivity algorithm including a parameterization of the absorption in the continuum region. J Atmos Sci 40:230–244

Giorgi F, Bi X (2000) A study of internal variability of regional climate model. J Geophys Res 105:29503–29521

Giorgi F, Jones C, Asrar G (2009) Addressing climate information needs at the regional level: the CORDEX framework. WMO Bull 58:175–183

Grell GA (1993) Prognostic evaluation of assumptions used by cumulus parameterizations. Mon Weather Rev 12:764–787

Grell GA, Dudhia J, Stauffer DR (1994) A description of the fifth generation penn system/NCAR mesoscale model (MM5). NCAR Tech Note NCAR/TN–398 + 1A

Hawkins E, Sutton R (2009) The potential to narrow uncertainty in regional climate predictions. Bull Am Meteorol Soc 90:1095–1107

Hewitt CD (2005) The ENSEMBLES project: providing ensemble-based predictions of climate changes and their impacts. Published article appears in the EGGS newsletter 13:22–25

Hsie EY, Anthes RA, Keyser D (1984) Numerical simulation of frontogenesis in a moist atmosphere. J Atmos Sci 41:2581–2594

Jones D, Simmonds I (1993) Time and space spectral analyses of southern hemisphere sea level pressure variability. Mon Weather Rev 121:661–672

Kain JS (2004) The Kain–Fritsch convective parameterization: an update. J Appl Meteorol 43:170–181

Kain JS, Fritsch JM (1993) Convective parameterization for mesoscale models: the Kain–Fritsch scheme. The representation of cumulus convection in numerical models. Meteor Monogr No 24, Amer Meteor Soc 165–170

Lucas-Picher P, Caya D, de Elía R, Laprise R (2008) Investigation of regional climate models' internal variability with a ten-member ensemble of 10-year simulations over a large domain. Clim Dyn 31:927–940

Lynn B, Healy R, Druyan LM (2009) Quantifying the sensitivity of simulated climate change to model configuration. Clim Change 92:275–298

Marengo JA, Ambrizzi T, da Rocha R, Cuadra SV, Alves LM, Valverde MC, Torres RR, Santos DC, Ferraz S (2010) Future change of climate in South America in the late twenty-first century: intercomparison of scenarios from three regional climate models. Clim Dyn 35:1089–1113

Mearns et al (2005) NARCCAP (North American Regional Climate Change Assessment Program). A multiple AOGCM and RCM climate scenario project over North America. In: AMS 16th conference on climate variations and change, pp 235–238

Mellor GL, Yamada T (1974) A hierarchy of turbulence closure models for planetary boundary layers. J Atmos Sci 31:1791–1806

Miguez-Macho G, Stenchikov G, Robock A (2005) Regional climate simulations over North America: interaction of local processes with improved large-scale flow. J Clim 18:1227–1246

Murphy JM, Sexton DMH, Barnett DN, Jones GS, Webb MJ, Collins M, Stainforth DA (2004) Quantification of modelling uncertainties in a large ensemble of climate change simulations. Nature 429:768–772

Murphy JM, Booth BB, Collins M, Harris GR, Sexton DMH, Webb MJ (2007) A methodology for probabilistic predictions of regional climate change from perturbed physics ensembles. Phil Trans R Soc A 365:1993–2028

Nogués-Paegle J, Mo KC (1997) Alternating wet and dry conditions over South America during summer. Mon Weather Rev 125:279–291

Nuñez MN, Solman S, Cabré MF (2009) Regional Climate change experiments over Southern South America. II: climate change scenarios in the late twenty first century. Clim Dyn 32:1081–1095

O'Brien T, Sloan LC, Snyder MA (2010) Can ensembles of regional climate model simulations improve results from sensitivity studies? Clim Dyn. doi:10.1007/s00382-010-0900-5

Rauscher S, Seth A, Qian J-H, Camargo SJ (2006) Domain choice in a an experimental nested modeling prediction system for South America. Theor Appl Climatol 86:229–246

Rinke A, Dethloff K, Cassano JJ, Christensen JH, Curry JA, Du P, Girard E, Haugen JE, Jacob D, Jones CG, Køltzow M, Laprise R, Lynch AH, Pfeifer S, Serreze MC, Shaw MJ, Tjernström M, Wyser K, Zagar M (2006) Evaluation of an ensemble of Arctic regional climate models: spatiotemporal fields during the SHEBA year. Clim Dyn 6:459–472

Sanchez E, Berbery E, Solman S, García-Ochoa R, Samuelsson P, Remedio A, Jacob D, Rojas M, Sörensson A, Menendez C, Porfirio da Rocha R, Castro M, Pessacg N, Marengo J, Chan Chou S, Li L, Le Treut H (2010) Present climate validation of an ensemble of regional climate models over South America forced by 1989–2008 ERAinterim reanalysis. Eos Trans AGU 91(26) Meet Am Suppl, Abstract GC33A-02

Seth A, Giorgi F (1998) The effects of domain choice on summer precipitation simulation and sensitivity in a regional climate model. J Clim 11:2698–2712

Seth A, Rojas M (2003) Simulation and sensitivity in a nested modeling system for South America. Part I. Reanalysis boundary forcing. J Clim 16:2437–2453

Solman S, Pessacg N (2011) Regional climate simulations over South America: sensitivity to model physics and to the treatment of lateral boundary conditions using the MM5 model. Clim Dyn. doi:10.1007/s00382-011-1049-6

Stephens GL (1978) Radiation profiles in extended water clouds: II. Parameterization schemes. J Atmos Sci 35:2123–2132

Tadross M, Gutowski W, Hewitson W, Jack C, New M (2006) MM5 simulations of interannual change and the diurnal cycle of southern African regional climate. Theor Appl Climatol 86:63–80

Uppala SM et al (2005) The ERA-40 re-analysis. Q J R Meteorol Soc 131:2961–3012. doi:10.1256/qj.04.176

Vanvyve E, Hall N, Messager C, Leroux S, van Ypersele JP (2008) Internal variability in a regional climate model over West Africa. Clim Dyn 30:191–202

Wu W, Lynch AH, Rivers A (2005) Estimating the uncertainty in a regional climate model related to initial and lateral boundary conditions. J Clim 18:917–933

Yang Z, Arrit R (2002) Test of a perturbed physics ensemble approach for regional climate modeling. J Clim 15:2881–2896